Applied Microbiology and Biotechnology (2021) 105:7871–7888
https://doi.org/10.1007/s00253-021-11581-8

GENOMICS, TRANSCRIPTOMICS, PROTEOMICS

# Antifungal mechanism of 1-nonanol against *Aspergillus flavus* growth revealed by metabolomic analyses

**Shuai-Bing Zhang[1,2] · Yu-Liang Qin[1,2] · Sheng-Fa Li[1,2] · Yang-Yong Lv[1,2] · Huan-Chen Zhai[1,2] · Yuan-Sen Hu[1,2] · Jing-Ping Cai[1,2]**

Received: 5 June 2021 / Revised: 5 September 2021 / Accepted: 8 September 2021 / Published online: 22 September 2021


## Abstract

Chemical control of fungal spoilage of postharvest cereal grains is an important strategy for the management of grain storage. Here, the potential antifungal activity of 1-nonanol, a main component of cereal volatiles, against *Aspergillus flavus* was studied. The growth of *A. flavus* was completely inhibited by 0.11 and 0.20 μL/mL 1-nonanol at vapor and liquid contact phases, respectively. Metabolomic analysis identified 135 metabolites whose expression was significantly different between 1-nonanol-treated and untreated *A. flavus*. These metabolites were involved in the tricarboxylic acid cycle, amino acid biosynthesis, protein degradation and absorption, aminoacyl-tRNA biosynthesis, mineral absorption, and in interactions with ABC transporters. Biochemical validation confirmed the disruptive effect of 1-nonanol on *A. flavus* growth, as indicated by the leakage of intracellular electrolytes, decreased succinate dehydrogenase, mitochondrial dehydrogenase, and ATPase activity, and the accumulation of reactive oxygen species. We speculated that 1-nonanol could disrupt cell membrane integrity and mitochondrial function and might induce apoptosis of *A. flavus* mycelia. Simulated grain storage experiments showed that 1-nonanol vapor, at a concentration of 264 μL/L, completely inhibited *A. flavus* growth in wheat, corn, and paddy grain with an 18% moisture content. This study provides new insights into the antifungal mechanism of 1-nonanol against *A. flavus*, indicating that it has a promising potential as a bio-preservative to prevent fungal spoilage of postharvest grains.

### Key points

- *1-Nonanol showed higher antifungal activity against A. flavus.*
- *The antifungal mechanisms of 1-nonanol against A. flavus were revealed.*
- *1-Nonanol could damage cell membrane integrity and mitochondrial function.*

**Keywords** 1-Nonanol · *Aspergillus flavus* · Antifungal mechanism · Metabolomic analyses · Cereal grain

## Introduction

Cereal grains, such as ripe crop seeds, are the staple food for almost all of the world's population and are often stored for more than 1 year after harvest to supply cereal industries (Fleurat-Lessard 2017). Long-term stored cereal grains, especially in humid and hot climates, are often infected with seed-borne fungi, mainly of the *Aspergillus* and *Penicillium* species, which seriously deteriorate the quantity and quality of stored grains, and can even produce harmful mycotoxins (Mohapatra et al. 2017). Therefore, prevention of fungal spoilage of postharvest grains is critical for the economy and safety of cereal grains and their derived foods. Chemical control is an important alternative approach to prevent fungal spoilage of cereal grains (Magan and Aldred 2007). To our knowledge, propionic acid and its salts are the only cereal grain preservatives in preventing fungal spoilage of postharvest grain in several countries. There is a demand for more sustainable, safe, and efficient alternative preservatives for the postharvest management of cereal grains.

✉ Shuai-Bing Zhang
shbzhang@163.com

[1] College of Biological Engineering, Henan University of Technology, 100 Lianhua Street, Zhengzhou 450001, People's Republic of China

[2] Henan Provincial Key Laboratory of Biological Processing and Nutritional Function of Wheat, Zhengzhou 450001, People's Republic of China

Plant volatiles are a complex mixture of lipophilic secondary metabolites with high vapor pressure that serve multiple physiological functions in producer organs (Pichersky et al. 2006). With the increase in volatile compounds with defensive functions discovered, plant volatiles are now considered a chemical weapon against pathogens or predators (Maffei et al. 2011). The biotechnological potential of plant volatiles as a natural and eco-friendly solution to defend against pathogens has attracted increasing attention (Brilli et al. 2019; Hammerbacher et al. 2019; Ma and Johnson 2021; Mari et al. 2016; Obianom and Sivakumar 2018). A variety of volatiles, including aldehydes, alcohols, and acids, can be produced from postharvest cereal grains through the lipoxygenase pathway, which is the chemical basis for the flavor of cereal grains (Buttery et al. 1978; Mattiolo et al. 2017; Yang et al. 2008; Zhou et al. 1999). Of these volatile organic compounds, propionic acid and hexanal are promising fungicidal fumigants for the management of stored agricultural commodities (Dhakshinamoorthy et al. 2020; Kabak et al. 2006; Zhang et al. 2021a). Further exploitation of cereal volatiles with antifungal potency could provide an interesting approach for the chemical control of fungal spoilage of cereal grains.

1-Nonanol is one of the main components of wheat volatiles, which was found to have considerable antimicrobial activity (Mattiolo et al. 2017). It has been reported that 1-nonanol showed the highest inhibitory activity against the growth of postharvest fungal pathogen *Geotrichum candidum* citrus race among the straight-chain (C6-C12) alcohols (Suprapta et al. 1997). 1-Nonanol can inhibit *Mycobacterium smegmatis* and *Mycobacterium tuberculosis* by damaging their cell envelope (Mukherjee et al. 2013) and has bactericidal activity and membrane-damaging activity against *Staphylococcus aureus* (Togashi et al. 2007). Additionally, 1-nonanol inhibits the growth of *Saccharomyces cerevisiae* and *Zygosaccharomyces bailii* by disrupting the membrane-associated function of integral proteins (Kubo and Cespedes 2013). As a cereal-derived volatile and an authorized food additive by the National Health and Family Planning Commission of China (Chinese Standards for Food Additives GB2760-2014), 1-nonanol shows great potential as a preservative in preventing fungal spoilage of cereal grains. However, there are few reports about the fungicidal activity of 1-nonanol against spoilage fungi in cereal grains.

In this study, to reveal the antifungal effect of 1-nonanol against *A. flavus*, (1) the fungicidal potency of 1-nonanol against the growth of *A. flavus* on agar plates and liquid medium was evaluated at the vapor and liquid contact phases; (2) the primary antifungal mechanisms of 1-nonanol against *A. flavus* were investigated through metabolomic analyses and biochemical validation; (3) the effectiveness of 1-nonanol vapor against the growth of *A. flavus* in 18% moisture wheat, corn, and paddy grains was determined. This study provides an experimental foundation for the potential application of 1-nonanol as a biopreservative in cereal grains.

## Materials and methods

### Materials and chemicals

*A. flavus* NRRL 3357 strain was cultured on potato dextrose agar (PDA) medium (200 g/L potato infusion, 20 g/L glucose, and 15 g/L agar) at 28 ± 1 °C for 5 days before use. 1-Nonanol (cas: 205–583-7, 98%) was purchased from Macklin (Shanghai, China). HPLC-grade ammonium hydroxide and ammonium acetate were purchased from Sigma-Aldrich (St. Louis, MO, USA). Menadione and XTT sodium salts (2,3-bis[2-methoxy-4-nitro-5-sulphophenyl]-2H-tetrazolium-5-carboxanilide) were purchased from Sigma Chemical Co., Ltd. (Shanghai, China). Succinate dehydrogenase (SDH) and ATPase assay kits were purchased from Jiancheng Bioengineering Institute (Nanjing, Jiangsu, China). Assay kits for superoxide anion and $H_2O_2$ were purchased from Sigma-Aldrich (St. Louis, MO, USA). Wheat, corn, and paddy grain were purchased from local market.

### Effect of 1-nonanol on the growth of *A. flavus* on agar plate

The effect of 1-nonanol on the growth of *A. flavus* was determined by vapor fumigation (Zhang et al. 2021a, b). *A. flavus* spore suspension $5 \times 10^6$ spores/mL was prepared by dissolving spores in sterile saline containing 0.1% (v/v) Tween 80 and counted with a hemocytometer, and 1 μL was inoculated onto a PDA plate. Different concentrations of 1-nonanol (0, 0.03, 0.05, 0.08, and 0.11 μL/mL) were added to the lid of the Petri dishes, which were sealed with Parafilm. The cultures were incubated at 28 ± 1 °C for 5 days, and the colony diameter was measured daily after the third day. The lowest 1-nonanol concentration that did not result in visible *A. flavus* growth was considered the minimum inhibitory concentration (MIC). Then, the 1-nonanol vapor in the glass Petri dishes, in which the growth of *A. flavus* had been completely inhibited, was replaced with sterile air and cultured for another 3 days. The lowest concentration at which no growth occurred after the final 3-day incubation was determined as the minimal fungicidal concentration (MFC).

### Effect of 1-nonanol on the growth of A. flavus in liquid medium

Different concentrations of 1-nonanol (0, 0.025, 0.05, 0.075, 0.1, 0.15, and 0.20 μL/mL) were added to 100 mL yeast extract medium with supplements (YES, 20 g/L yeast extract, 0.5 g/L magnesium sulfate, 20 g/L sucrose). One milliliter suspension of *A. flavus* spores ($5 \times 10^6$ spores/mL) was inoculated into the liquid medium and cultivated at 28 ± 1 °C on a rotary shaker at 200 revolutions per minute (rpm) for 5 days. *A. flavus* mycelia were recovered after filtering through pre-weighed filter paper and washed three times with sterile water. The filter paper with the mycelia was dried at 80 °C for 6 h, and then the net dry weight of mycelia was determined. All tests were performed in triplicate.

### Effect of 1-nonanol on cell membrane leakage

One milliliter suspension of *A. flavus* spores ($5 \times 10^6$ /mL) was inoculated into 100 mL YES medium and cultivated for 3 days at 28 ± 1 °C and 200 rpm. Then, 20 μL 1-nonanol was added to treat *A. flavus* cultures, and untreated cultures were used as controls. The culture broth was removed at intervals and centrifuged at 4000 × *g* for 10 min to recover the supernatant. Cell membrane leakage was examined by measuring the electrical conductivity and optical absorption of the culture supernatant at 260 nm ($A_{260nm}$) according to previously reported methods (Shao et al. 2013). The integrity of plasma membrane in *A. flavus* mycelia was observed with confocal laser scanning microscope (CLSM FV3000, Olympus Corporation, Japan). The hyphae were stained with prodium iodide (PI) using plasma membrane detection kit (Solarbio Science & Technology Co., Ltd., Beijing, China). All experiments were repeated three times.

### LC–MS/MS analysis

*A. flavus* cultures were cultivated as described above for 3 days. 1-Nonanol was added to the culture to a final concentration of 0.20 μL/mL. After incubation for another 6 h, *A. flavus* mycelia were collected, washed three times with 0.1 M phosphate buffer solution (PBS; pH 7.4), and immediately frozen in liquid nitrogen. Samples were stored at − 80 °C. An *A. flavus* culture without 1-nonanol treatment was used as a control. Six parallel samples were prepared for LC–MS/MS analysis. After the sample was slowly thawed at 4 °C, 100 mg (wet weight) of mycelia was mixed with 200 pre-cooled methanol/acetonitrile/water solution (2:2:1, v/v) and homogenized at 4 °C for 30 min. The cell lysate was centrifuged at 14,000 × *g* at 4 °C for 20 min and kept at − 20 °C for 10 min, after which the supernatant of cell lysate was recovered and freeze-dried under vacuum. The dried composition was dissolved in 100 μL of acetonitrile solution (acetonitrile: water, 1:1, v/v), vortexed to mix, and centrifuged at 14,000 × *g* at 4 °C for 15 min before mass spectrometry analysis.

The samples were analyzed using ultra-high performance liquid chromatography (UHPLC, 1290 Infinity LC, Agilent Technologies, Palo Alto, CA, USA) coupled with a Triple TOF 6600 mass spectrometer (AB SCIEX, Framingham, MA, USA). A 2 μL sample was injected and separated using an ACQUITY UPLC BEH amide column (1.7 μm, 2.1 × 100 mm, Waters, Milford, MA, USA) at 25 °C column temperature. A flow rate of 0.5 mL/min was applied with the mobile phase consisting of solution (A) (aqueous solution containing 25 mM ammonium acetate and 25 mM ammonia) and solution (B) acetonitrile. The gradient elution procedure was as follows: 0–0.5 min, 95% B; 0.5–7 min, 95 to 65% B; 7–8 min, 65 to 40% B; 8–9 min, 40% B; 9–9.1 min, 40 to 95% B; and 9.1–12 min, 95% B. The sample was placed in a 4 °C autosampler during the entire analysis. To avoid the influence of fluctuations in the detection signal of the instrument, a random order was adopted for the sample analysis. Quality control (QC) samples were analyzed to monitor and evaluate the stability of the system and the reliability of the experimental data.

Electrospray ion source conditions were as follows: ion source gas 1, 60; ion source gas 2, 60; curtain gas, 30; source temperature, 600 ℃; IonSapary Voltage Floating ± 5500 V (both positive and negative modes); TOF MS scan m/z range, 60–1000 Da; product ion scan m/z range, 25–1000 Da; TOF MS scan accumulation time, 0.20 s/spectra; and product ion scan accumulation time, 0.05 s/spectra. The secondary mass spectrum was acquired by information-dependent acquisition (IDA) and adopted a high sensitivity mode; declustering potential (DP), ± 60 V (both positive and negative modes); and collision energy, 35 ± 15 eV. IDA settings were as follows: exclude isotopes within 4 Da and candidate ions to monitor per cycle, 10.

### Data processing

The original data were converted into a MzXML format by Proteo Wizard (http://proteowizard.sourceforge.net/), and the peak alignment, retention calibration, and extraction of peak area were analyzed using XCMS (https://xcmsonline.scripps.edu). Metabolite structure identification, data preprocessing, and quality evaluation were performed based on the data extracted by XCMS. Finally, univariate statistical analysis, multi-dimensional statistical analysis, differential metabolite screening, correlation analysis of differential metabolites, and KEGG pathway analysis were performed. Exact mass number matching (< 25 PPM) and secondary spectrum matching were conducted by searching the internal database (Shanghai Applied Protein Technology Co., Ltd., Shanghai, China).

### Determination of SDH, mitochondrial dehydrogenase, and ATPase activity

*A. flavus* was cultivated in YES medium for 3 days and exposed to 0.20 µL/mL 1-nonanol for another 6 h. *A. flavus* mycelia were collected and washed three times with 0.1 M PBS (pH 7.4). Untreated cultures were used as controls. Wet mycelia (0.1 g) were ground in liquid nitrogen and re-suspended in 1 mL 0.1 M PBS (pH 7.4). The supernatant was recovered for biochemical analysis after centrifugation at 12,000 × *g* for 15 min at 4 °C. SDH activity in the supernatant was determined following the manufacturer's instructions. SDH activity was detected at 600 nm in redox reaction assays. The activity of mitochondrial dehydrogenase in the supernatant was detected using the XTT method (Zhang et al. 2021b). Briefly, a final concentration of 50 µg/mL XTT and 25 µM menadione was added to a 96-well microplate, and 200 µL of supernatant was added to the reaction solution and incubated at 37 °C for 2 h. The optical absorption of the orange-colored formazan product in the reaction solution was measured at 450 nm using a microplate reader (Tecan Spark 10 M, Tecan Trading AG, Männedorf, Switzerland). All tests were performed in triplicate. ATPase activity was monitored to evaluate the inhibition of 1-nonanol on *A. flavus* following the manufacturer's protocol. The absorbance values of all samples were measured at 660 nm.

### Determination of reactive oxygen species (ROS) accumulation

The recovered supernatant of *A. flavus* homogenate was used to determine the $H_2O_2$ and superoxide anion content in *A. flavus* cells using a $H_2O_2$ and superoxide anion assay kit, respectively, according to the manufacturer's instructions. All tests were performed in triplicate. ROS accumulation in *A. flavus* mycelia was observed with CLSM after the mycelia were stained with DCFH-DA (2′,7′-dichlorofluorescin diacetate) probe, a redox-sensitive fluorescent, using the ROS assay kit (Solarbio Science & Technology Co., Ltd. Beijing, China). Three independent replicates were performed for each treatment.

### 1-Nonanol fumigation of grains under simulated storage conditions

The control effectiveness of 1-nonanol vapor against *A. flavus* in high-moisture wheat, corn, and paddy grains was evaluated under simulated storage conditions. The grain kernels were immersed in a 1% sodium hypochlorite solution for 2 min and washed 3 times with sterile water. The washed grains were dried at 60 °C for 6 h under aseptic conditions. The moisture content of the grains was adjusted to 18.0% by spraying sterile distilled water and then equilibrated under air-tight aseptic conditions at 4 °C for 24 h. Then, *A. flavus* spores were mixed with the 18% moisture grains to approximately $10^3$ spores per gram. The grains (200 g) were loaded into a 300 mL air-tight plastic bottle and fumigated with 0, 44, 88, 176, and 264 µL/L 1-nonanol (Zhang et al. 2021a). The fumigated grains were stored in a Binder KBF720 climatic chamber (Binder, Tuttlingen, Germany) at 28 ± 1 °C for 5 weeks. Subsequently, microbiological analyses were performed as previously described (Zhai et al. 2015). Briefly, 25 g of stored grain was sampled and immersed in 225 mL of sterile distilled water in a 500 mL flask bottle and then shaken on a flatbed shaker at 300 excursions per min for 30 min. The sample solution was diluted $10^2$–$10^5$ times, and 1 mL of the diluted solution was inoculated into a sterile Petri dish and mixed with the modified Czapek's medium (30 g/L sucrose, 60 g/L NaCl, 1 g/L $K_2HPO_4$, 3 g/L $NaNO_3$, 0.5 g/L KCI, 0.5 g/L $MgSO_4 \cdot 7H_2O$, 20 g/L agar powder). After incubated at 28 ± 1 °C for 7 days, the *A. flavus* number was counted on the fifth day, and the fungal count in stored grains was calculated. All experiments were performed in triplicate.

### Statistical analysis

Multivariate data analysis, including Pareto-scaled principal component analysis (PCA) and orthogonal partial least-squares discriminant analysis (OPLS-DA), was performed using the R software (https://www.r-project.org/). The robustness of the model was evaluated through a sevenfold cross-validation and response permutation test. The contribution of each variable to the classification was calculated based on the variable importance in the projection (VIP) value in the OPLS-DA model. The significance of each metabolite was measured at the univariate level by a Student's *t*-test of the metabolites with a VIP value > 1 and $p < 0.05$, which was considered statistically significant. The volcano map was drawn based on the *t*-test and multiple variation analysis of metabolites using R software. Biochemical data were analyzed with one-way analysis of variance (ANOVA) using SPSS 20.0 (IBM, Armonk, NY, USA), and differences with a *p*-value of < 0.05 were considered statistically significant. All biochemical data analyses were performed in triplicate.

## Results

### Inhibition effect of 1-nonanol on the growth of A. flavus

1-Nonanol inhibited the growth of *A. flavus* in a dose-dependent manner (Fig. 1A, B). The colony diameter of *A. flavus* was negatively correlated with an increase of the 1-nonanol vapor concentration (Fig. 1A, B), and the MIC and MFC of 1-nonanol

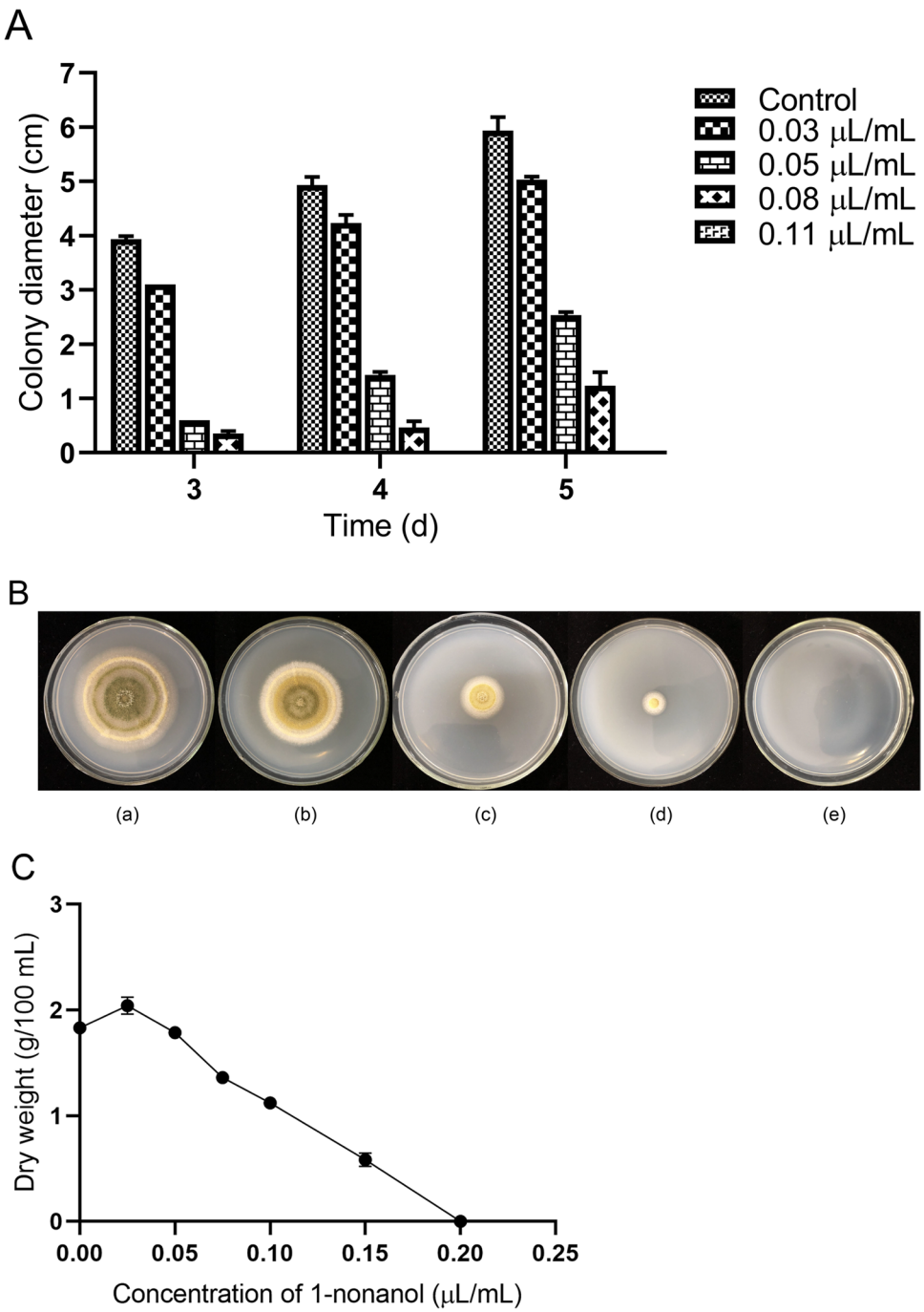


**Fig. 1** Effect of 1-nonanol on the growth of *Aspergillus flavus* mycelium. (A) Change in colony diameters of *A. flavus* grown on PDA medium treated with different concentrations 1-nonanol vapor over time. (B) *A. flavus* colonies fumigated with (a) 0, (b) 0.03, (c) 0.05, (d) 0.08, and (e) 0.11 μL/mL 1-nonanol vapor on the 5th day of cultivation. (C) Dry weight of *A. flavus* mycelia cultivated in YES liquid medium with or without different concentrations 1-nonanol on the 5th day of cultivation

vapor against *A. flavus* were 0.11 and 0.19 μL/mL, respectively. When *A. flavus* was cultivated in liquid YES medium, 0.20 μL/mL 1-nonanol completely inhibited its growth (Fig. 1C).

## Effect of 1-nonanol on the plasma membrane leakage of A. flavus

Previous studies suggested that 1-nonanol could disrupt the membrane integrity of microbial cells (Kubo and Cespedes 2013; Mukherjee et al. 2013). The electrical conductivity and $A_{260nm}$ in the culture supernatant of *A. flavus* exposed to 0.20 μL/mL 1-nonanol were measured to evaluate plasma membrane leakage. Compared to the control sample, the extracellular conductivity and $A_{260nm}$ of the culture supernatant of 1-nonanol-treated *A. flavus* considerably increased during the first 6 h of incubation (Fig. 2A), which indicated that 1-nonanol could damage the plasma membrane of *A. flavus* and cause subsequent electrolyte leakage. The membrane damage of *A. flavus* mycelia exposure to 1-nonanol was visualized by confocal

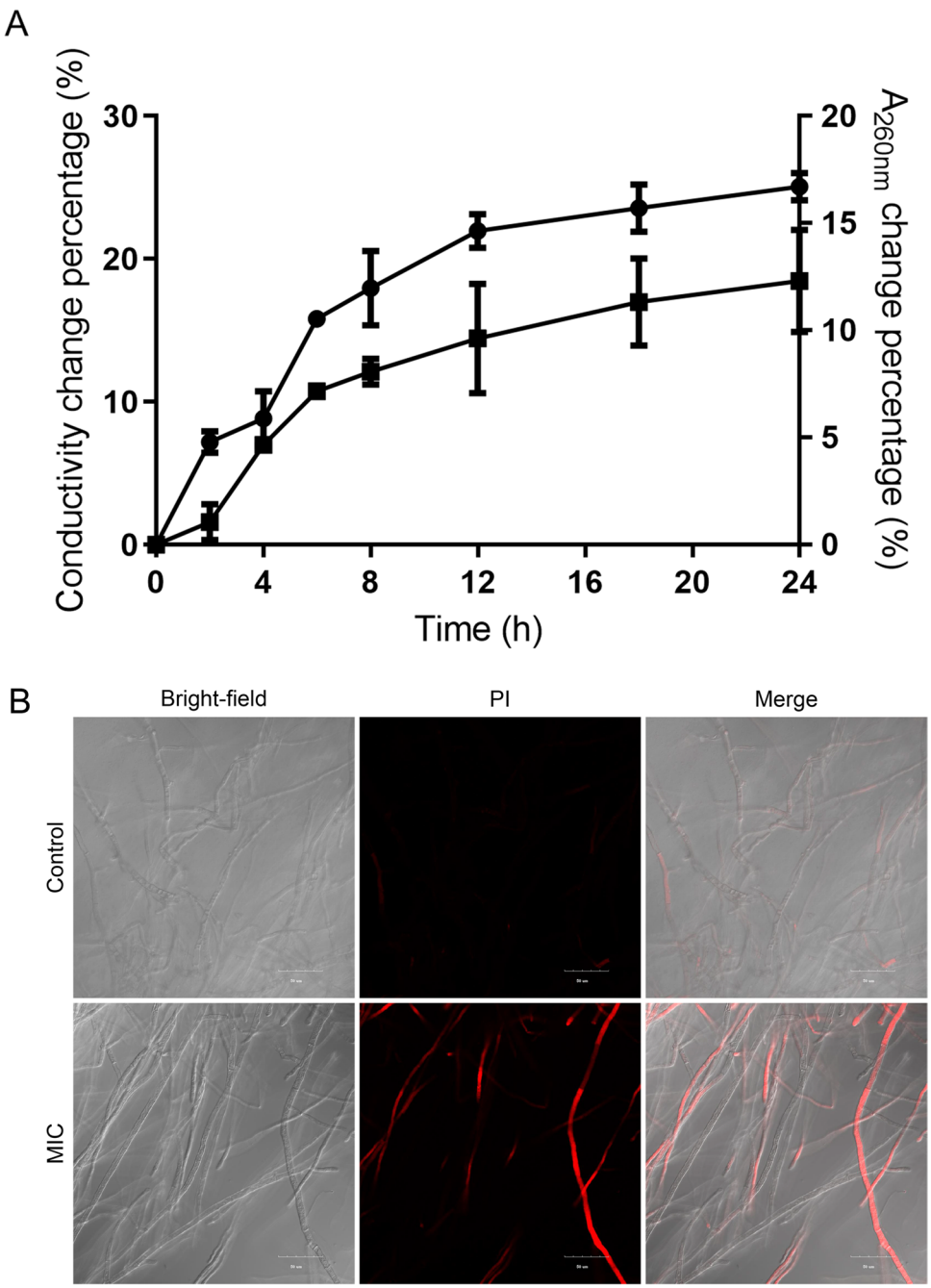


**Fig. 2** Effect of 1-nonanol on the plasma membrane leakage of *A. flavus*. **A** The conductivity change percentage (circles) and $A_{260nm}$ change percentage (squares) of culture supernatant of *A. flavus* after exposed to 0.20 μL/mL 1-nonanol. **B** Images obtained by confocal laser scanning microscope

laser scanning microscope after staining with PI. The results showed that the fluorescence density of 1-nonanol-treated mycelia was remarkably enhanced compared with that of the control group (Fig. 2B), which confirmed that 1-nonanol treatment can damage the membrane integrity of *A. flavus* mycelia. Therefore, the mycelium of *A. flavus* was collected for subsequent metabolomic analyses after being exposed to 0.20 μL/mL 1-nonanol for 6 h.

## Multivariate analysis

Extracts of 1-nonanol-treated and untreated *A. flavus* mycelia were analyzed in positive and negative ion modes using a UHPLC-Triple-TOF mass spectrometer. All potential differential metabolites identified were linearly recombined by PCA, and highly correlated metabolites were clustered together. The PCA scoring plots showed altered metabolite

levels in *A. flavus* mycelia after exposure to 1-nonanol in both the positive (Fig. 3A) and negative (Fig. 3B) ion patterns. To predict the metabolite type, potential biomarkers were identified using a supervised discriminant analysis statistical method (PLS-DA), and distinct cohorts of 1-nonanol-treated and untreated groups were divided according to metabolic differences into positive (Fig. 3C) and negative (Fig. 3D) ion modes, respectively. The predictability and reliability of the PL-SDA model were evaluated in the positive ($r^2 = 0.996$, $q^2 = 0.980$) and negative ($r^2 = 1.0$, $q^2 = 0.994$) ion modes, respectively. The relationship between sample category and metabolites in the positive ($r^2 = 0.996$, $q^2 = 0.978$) (Fig. 3E) and negative (Fig. 3F) ($r^2 = 1.0$, $q^2 = 0.992$) ion modes was established through a PLS-DA correction using OPLS-DA, which showed that the model is highly predictable and reliable.

## Univariate statistical analysis

The significance of metabolite changes between 1-nonanol-treated and untreated *A. flavus* mycelia was assessed by univariate statistical analysis. Volcano plots (Supplemental Fig. S1) were generated to represent the up- and downregulated metabolites in the positive (Supplemental Fig. S1 A) and negative (Supplemental Fig. S1 B) ion modes. The upregulated (FC > 1.5, $p < 0.05$) and downregulated (FC < 0.67, $p < 0.05$) metabolites were labeled as red and blue, respectively. Significantly differential metabolites (VIP > 1 and $p < 0.05$) and differential metabolites (VIP > 1 and $0.05 < p < 0.1$) between 1-nonanol-treated and control samples were categorized based on the contribution of each variable determined by importance in projection (VIP) scores after OPLS-DA. A total of 135 significantly differential metabolites were identified as the main factors separating the control and 1-nonanol-treated groups, whereas 87 upregulated metabolites and 48 downregulated metabolites were categorized (Table 1).

## Hierarchical clustering analysis

To evaluate the rationality of differential metabolites and visualize their relationships in a comprehensive manner, heatmaps of up- and downregulated significantly differential metabolites in *A. flavus* cells after exposure to 1-nonanol were assembled using hierarchical clustering analysis (Supplemental Fig. S2 A, B). Metabolites in the same cluster have similar expression patterns, perform similar functions, or participate in the same metabolic process or cellular pathway. KEGG enrichment analysis showed that the significantly differential metabolites were involved in the tricarboxylic acid cycle (TCA), amino acid biosynthesis, protein degradation and absorption, aminoacyl-tRNA biosynthesis, mineral absorption, and in interactions with ABC transporters (Fig. 4). These results indicate that multiple *A. flavus* metabolic pathways were regulated in response to 1-nonanol treatment. In the positive mode (Supplemental Fig. S2 A), *N*-ω-hydroxyarginine, tyramine, *trans*-vaccenic acid, xanthohumol, and acetylcarnitine were considerably upregulated, and inosine, isopentenyladenosine, L-glutamine, L-pyroglutamic acid, allopurinol riboside, L-pipecolic acid, and 1-palmitoyl-sn-glycero-3-phosphocholine were significantly downregulated in the 1-nonanol-treated sample. In the negative mode (Supplemental Fig. S2 B), glycyl-L-leucine, oleanolic acid, D-ribose, and DL-3-phenyllactic acid were upregulated, and L-glutamate, L-glutamine, dihydrothymine, 2-isopropylmalic acid, ribothymidine, inosine, and 1-palmitoyl-2-hydroxy-sn-glycero-3-phosphoethanolamine were downregulated in the 1-nonanol-treated sample. Succinate, a key intermediate product in the TCA pathway, decreased to 64.9% in 1-nonanol-treated *A. flavus* compared to the untreated control (Fig. 5). L-carnitine, stearidonic acid, and olinoleic acid, which are involved in fatty acid metabolism, were downregulated by 28.4%, 42.1%, and 57.7%, respectively, in *A. flavus* exposed to 1-nonanol. D-Mannitol, ribitol, L-fucose, and 2′-deoxy-D-ribose, which are related to carbohydrate metabolism, decreased to 49.1%, 48.4%, 46.5%, 41.3%, and 34.7%, respectively, in 1-nonanol-treated *A. flavus* compared to the untreated control.

## Effects of 1-nonanol on SDH, mitochondrial dehydrogenase, and ATPase activity

To confirm the effect of 1-nonanol on mitochondrial function and membrane transportation of *A. flavus*, the activities of SDH, mitochondrial dehydrogenase, and ATPase were compared between 1-nonanol-treated and untreated *A. flavus*. The activities of SDH, mitochondrial dehydrogenases, and ATPase were significantly reduced in 1-nonanol-treated *A. flavus* (Fig. 6). After exposure to 0.20 μL/mL 1-nonanol for 6 h, SDH activity in *A. flavus* mycelia reduced from $20.4 \pm 1.6$ to $12.6 \pm 0.5$ U/g. Mitochondrial dehydrogenase activity in 1-nonanol-treated *A. flavus* decreased by approximately 25.4 in comparison with the untreated sample. ATPase activity in *A. flavus* mycelia was downregulated from $16.6 \pm 0.2$ to $9.4 \pm 0.1$ U/mg.

## Effects of 1-nonanol on the reactive oxygen species level

$H_2O_2$ and superoxide anion levels were assessed to determine the effect of 1-nonanol on oxidative stress in *A. flavus*. The levels of $H_2O_2$ and superoxide anion in untreated *A. flavus* cells were $0.81 \pm 0.02$ and $0.32 \pm 0.04$ molμ/g,

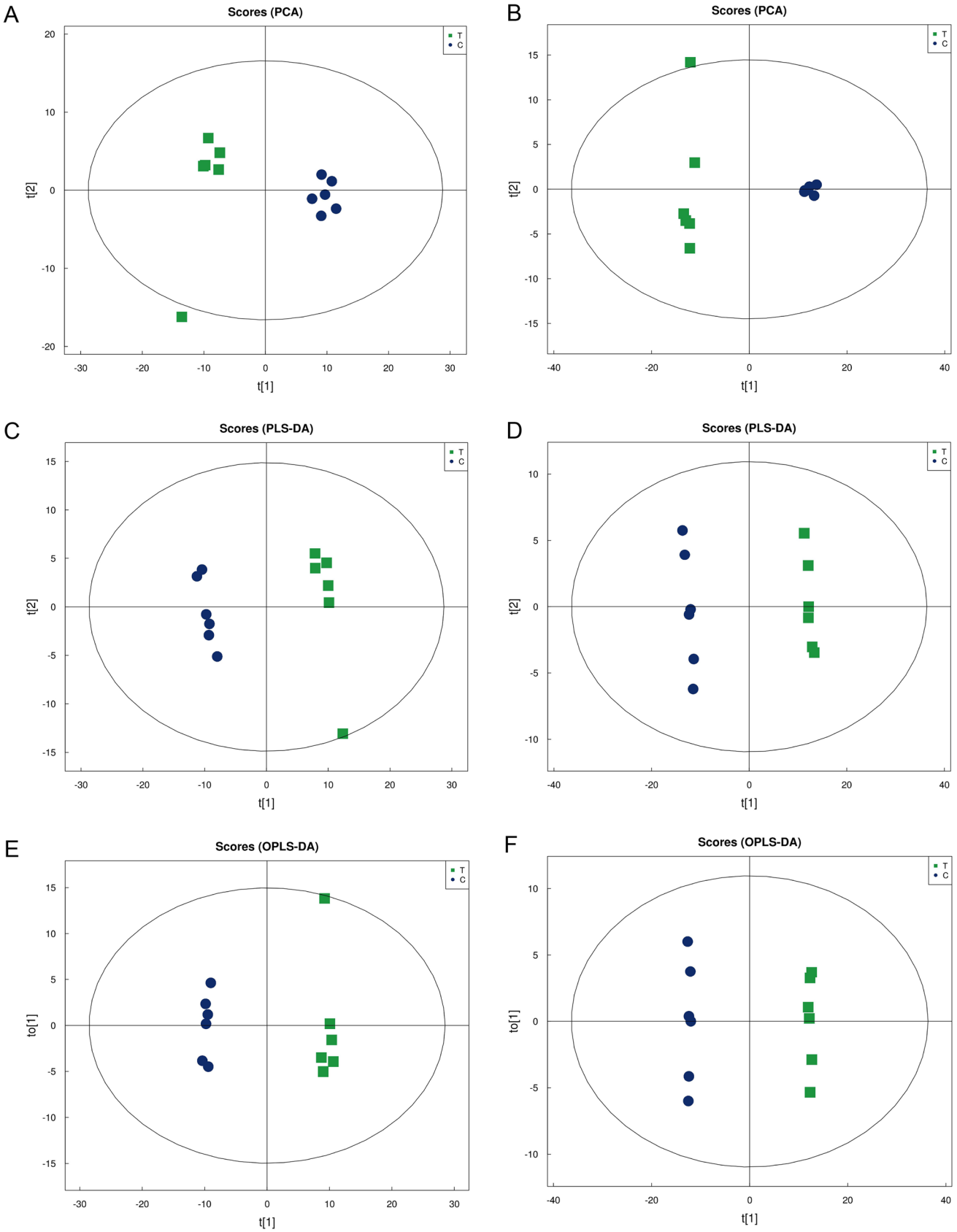
A
Scores (PCA)
T
C
t[2]
t[1]
B
Scores (PCA)
T
C
t[2]
t[1]
C
Scores (PLS-DA)
T
C
t[2]
t[1]
D
Scores (PLS-DA)
T
C
t[2]
t[1]
E
Scores (OPLS-DA)
T
C
to[1]
t[1]
F
Scores (OPLS-DA)
T
C
to[1]
t[1]

◂**Fig. 3** Score plots of PCA, PLS-DA, and OPLS-DA based on the UHPLC-Triple-TOF MS spectra. 1-Nonanol-treated (green dots) and untreated (blue dots) *A. flavus* are shown in positive mode (**A**, **C**, and **E**) and negative mode (**B**, **D**, and **F**). T, 1-nonanol-treated sample; C, untreated sample

respectively. However, $H_2O_2$ and superoxide anion levels in 1-nonanol-treated *A. flavus* cells increased to $2.03 \pm 0.08$ and $0.71 \pm 0.03$μ mol/g, respectively (Fig. 7). The results indicated that 1-nonanol induced higher oxidative stress in *A. flavus* mycelia. The results of DCFH-DA staining showed that the fluorescence density of 1-nonanol-treated *A. flavus* mycelia was remarkably higher than that of the control group (Fig. 8), indicating increased ROS accumulation in *A. flavus* exposure to1-nonanol.

### Controlling efficacy of 1-nonanol against A. flavus growth in stored grains

To evaluate the antifungal efficacy of 1-nonanol against *A. flavus* spoilage of agricultural products, vapor fumigation was applied to sterilized 18% moisture wheat, corn, and paddy grains inoculated with *A. flavus* spores under simulated storage conditions. After a 5-week storage period, 1-nonanol showed efficient inhibitory potency against *A. flavus* in cereal grains in a dose-dependent manner (Fig. 9). 1-Nonanol vapor completely inhibited the growth of *A. flavus* in wheat, corn, and paddy grains at a concentration of 264 μL/L, demonstrating the promising applications of 1-nonanol as a biofumigant for the control of fungal spoilage in stored grains.

## Discussion

In the present study, we determined the effectiveness of 1-nonanol at inhibiting the growth of *A. flavus* both as a vapor and liquid contact phase. 1-Nonanol displayed higher inhibitory activity against *A. flavus* than the natural antifungal compounds cinnamaldehyde and citral (Liang et al. 2015; Qu et al. 2019), indicating its higher antifungal potency against *A. flavus* as a natural preservative. The primary inhibitory mechanism of 1-nonanol against *A. flavus* was studied using metabolomic analysis. And it was found that significantly differential metabolites were involved in multiple metabolic pathways in the *A. flavus* hyphae. 1-Nonanol fumigation of cereal grain showed its higher controlling efficacy against *A. flavus* growth.

The cell membrane mediates selective nutrient uptake and/or metabolite secretion in fungi (Rest et al. 1995). The permeability and integrity of the cytoplasmic membrane are essential for maintaining fungal viability. Treatment with several plant-derived antifungal products, such as tea tree oil, citronellal, and hexanal, can damage the fungal membrane permeability and increase the release of cellular material (Shao et al. 2013; Xu et al. 2021; Wu et al. 2016). In this study, 1-nonanol led to an increase in extracellular conductivity and $A_{260nm}$ in *A. flavus* culture, indicating that electrolyte leakage had occurred owing to reduced membrane integrity. PI staining results also confirmed that 1-nonanol treatment damaged the membrane integrity of *A. flavus* hyphae. A previous study suggested that alkanols, as nonionic surfactants, could disrupt the function of integral proteins, such as ATPases, ion channels, and transport proteins, in the membranes of *S. cerevisiae*, in an unspecific manner (Kubo and Cespedes 2013). The $H^+$-ATPase of the plasma membrane plays a critical role in the regulation of energy-dependent uptake of fungal metabolites such as sugars, amino acids, and minerals (Nakamoto and Slayman 1989). In this study, ATPase activity was reduced to 63.2% in *A. flavus* after exposure to 1-nonanol. The significantly differential metabolites associated with mineral absorption might be related to this reduction in ATPase activity in 1-nonanol-treated *A. flavus*. ABC transporters are a family of membrane-bound proteins that transport different molecules, including natural metabolites and various xenobiotics, across biological membranes. ABC proteins perform their ATP-driven transmembrane transport function to regulate cellular processes (Výglaš and Olejníková 2021). Significantly differential metabolites related to ABC transporters also indicated that 1-nonanol treatment damaged the permeability and integrity of the cytoplasmic membrane by disrupting normal ABC transporter function (Gupta et al. 2021; Sipos and Kuchler 2006; He et al. 2019).

Mitochondria are involved in multiple cellular processes in eukaryotic cells, including energy production, calcium homeostasis, aging, and apoptosis (Basse 2010). Mitochondrial dysfunction results in metabolic disorders and in an excess of reactive oxygen species (ROS) (Breitenbach et al. 2014). The TCA cycle is a central metabolic pathway that occurs in fungal mitochondria and connects the metabolic pathways of gluconeogenesis, transamination, deamination, and lipogenesis (Akram 2014). The up- or downregulation of intermediates in the TCA cycle leads to metabolic changes in carbohydrates, fatty acids, and amino acids (Wang et al. 2020). In this study, tens of up- or downregulated metabolites in amino acid and fatty acid biosynthesis pathways were directly or indirectly linked with intermediate products of the TCA cycle. Succinate, a key intermediate product in the TCA cycle, was downregulated in *A. flavus* exposed to 1-nonanol, indicating that 1-nonanol treatment might impair the mitochondria. The significantly decreased activities of SDH and mitochondrial dehydrogenase confirmed the disruption of the TCA cycle in *A. flavus* by 1-nonanol. Mitochondrial dysfunction can reduce electron transport effectiveness and generate more intracellular ROS, which would

**Table 1** Identification and variation of significantly differential metabolites in 1-nonanol treated *A. flavus* mycelia

| Adduct | Description | VIP | Fold change | *p*-value | m/z | Trend | Functional category |
|---|---|---|---|---|---|---|---|
| (M + H) + | Pro-Thr | 2.499 | 8.071 | 4.81E − 13 | 217.117 | ↑ | Others |
| (M + H) + | His-Val | 1.523 | 5.873 | 1.34E − 12 | 255.144 | ↑ | Others |
| (M + H) + | Pro-Glu | 2.756 | 8.725 | 6.36E − 12 | 245.112 | ↑ | Others |
| (M + H) + | Val-Lys | 1.095 | 4.285 | 9.05E − 12 | 246.180 | ↑ | Others |
| (M + H) + | Tyramine | 1.284 | 6.859 | 1.26E − 11 | 138.090 | ↑ | Neuroactive ligand-receptor interaction |
| (M + H) + | Val-Arg | 2.209 | 8.843 | 5.98E − 11 | 274.186 | ↑ | Others |
| (M + H) + | Pro-Ser | 1.744 | 12.733 | 7.23E − 11 | 203.102 | ↑ | Others |
| (M + H) + | Isopentenyladenosine | 1.924 | 0.272 | 1.94E − 10 | 336.165 | ↓ | Others |
| (M + H) + | Phe-Pro | 1.706 | 4.309 | 3.72E − 10 | 263.139 | ↑ | Others |
| (M + H) + | His-Tyr | 1.165 | 6.230 | 4.85E − 10 | 319.138 | ↑ | Others |
| (M + H) + | Ile-Asn | 1.773 | 5.157 | 5.76E − 10 | 246.144 | ↑ | Others |
| (2 M + H) + | L-pipecolic acid | 1.885 | 0.154 | 6.63E − 10 | 259.164 | ↓ | Lysine degradation |
| (M + H) + | Phe-Arg | 1.452 | 4.073 | 8.72E − 10 | 322.186 | ↑ | Others |
| (M + H) + | Thr-Leu | 1.971 | 10.061 | 9.02E − 10 | 233.148 | ↑ | Others |
| (M + H) + | *N*–αacetyl-L-arginine | 1.711 | 2.147 | 1.48E − 09 | 217.128 | ↑ | Others |
| (M + H) + | Ile-Thr | 2.002 | 8.665 | 1.51E − 09 | 233.149 | ↑ | Others |
| (M + H) + | L-proline | 8.980 | 2.196 | 1.52E − 09 | 116.071 | ↑ | ABC transporters |
| (M + $CH_3CN$ + Na) + | Triethanolamine | 1.375 | 3.023 | 1.53E − 09 | 213.122 | ↑ | Glycerophospholipid metabolism |
| (M + Na) + | Leu-Leu | 1.224 | 7.505 | 2.10E − 09 | 267.166 | ↑ | Others |
| (M + H) + | Val-Ile | 5.236 | 10.667 | 2.56E − 09 | 231.170 | ↑ | Others |
| (M + H) + | Leu-Gln | 1.939 | 6.214 | 4.10E − 09 | 260.159 | ↑ | Others |
| (M + H) + | Val-Val | 1.914 | 9.493 | 4.19E − 09 | 217.154 | ↑ | Others |
| (M + H) + | Arg-Ile | 2.868 | 8.057 | 4.38E − 09 | 288.202 | ↑ | Others |
| (M + H) + | Ala-Ile | 2.220 | 6.935 | 4.87E − 09 | 203.138 | ↑ | Others |
| (M + H) + | Cytosine | 2.882 | 4.319 | 5.80E − 09 | 112.049 | ↑ | Pyrimidine metabolism |
| (M + H-2$H_2O$) + | 2-Amino-2-methyl-1,3-propanediol | 5.338 | 2.102 | 6.46E − 09 | 70.065 | ↑ | Others |
| (M + H) + | Ile-Arg | 1.922 | 5.406 | 6.87E − 09 | 288.202 | ↑ | Others |
| (M + H) + | Ile-Glu | 1.838 | 4.292 | 1.26E − 08 | 261.144 | ↑ | Others |
| M + | 2-Methylbutyroylcarnitine | 3.514 | 0.338 | 1.36E − 08 | 246.169 | ↓ | Others |
| (M + $NH_4$) + | D-mannitol | 3.124 | 0.491 | 1.68E − 08 | 200.112 | ↓ | ABC transporters |
| (M + H) + | Acetylcarnitine | 6.466 | 2.891 | 2.75E − 08 | 204.123 | ↑ | Others |
| (M + H) + | Ile-Lys | 2.944 | 9.143 | 2.96E − 08 | 260.196 | ↑ | Others |
| (M + H) + | Xanthine | 2.122 | 2.111 | 4.10E − 08 | 153.040 | ↑ | Caffeine metabolism |
| (M + H) + | Ile-Met | 2.147 | 5.440 | 5.75E − 08 | 263.142 | ↑ | Others |
| (M + H) + | Stachyose | 1.406 | 1.717 | 5.78E − 08 | 667.226 | ↑ | Galactose metabolism |
| (M + H) + | Ala-Lys | 1.930 | 3.697 | 5.82E − 08 | 218.149 | ↑ | Others |
| (M + H) + | Ile-Leu | 6.119 | 12.319 | 8.57E − 08 | 245.185 | ↑ | Others |
| (M + H) + | Val-Pro | 1.367 | 4.772 | 1.69E − 07 | 215.138 | ↑ | Others |
| (M + H-$H_2O$) + | 1-Aminocyclopropanecarboxylic acid | 2.124 | 0.390 | 2.12E − 07 | 84.044 | ↓ | Cysteine and methionine metabolism |
| (M + H) + | D-proline | 1.156 | 3.316 | 2.86E − 07 | 116.069 | ↑ | Arginine and proline metabolism |
| (M + H) + | Tyr-Phe | 1.145 | 6.164 | 2.88E − 07 | 329.147 | ↑ | Others |
| (M + H) + | Ile-Trp | 2.648 | 12.458 | 4.20E − 07 | 318.180 | ↑ | Others |
| (M + H) + | Arg-Glu | 1.049 | 3.752 | 6.68E − 07 | 304.160 | ↑ | Others |
| (M + H) + | Pro-Ala | 2.036 | 7.113 | 7.84E − 07 | 187.107 | ↑ | Others |
| (M + H) + | γ-L-Glu–εL-Lys | 1.260 | 2.790 | 8.90E − 07 | 276.155 | ↑ | Others |
| (M + H) + | Ser-Lys | 1.290 | 3.242 | 1.07E − 06 | 234.144 | ↑ | Others |
| (M + H) + | Val-Phe | 3.237 | 8.604 | 1.50E − 06 | 265.154 | ↑ | Others |

**Table 1** (continued)

| Adduct | Description | VIP | Fold change | *p*-value | m/z | Trend | Functional category |
|---|---|---|---|---|---|---|---|
| $(M+NH_4)+$ | Maltopentaose | 12.971 | 1.484 | 1.66E−06 | 846.309 | ↑ | Others |
| (M + Na) + | *Trans*-vaccenic acid | 3.528 | 3.236 | 2.01E−06 | 305.246 | ↑ | Others |
| (M + H) + | Phe-Phe | 1.592 | 4.277 | 2.28E−06 | 313.153 | ↑ | Others |
| $(M+CH_3CN+H)+$ | Ergothioneine | 1.219 | 0.734 | 2.71E−06 | 272.133 | ↑ | Histidine metabolism |
| (M + H) + | Ile-Gly | 2.141 | 10.374 | 3.00E−06 | 189.122 | ↑ | Others |
| (M + H) + | 4-Aminobutyric acid | 3.660 | 1.420 | 3.34E−06 | 104.070 | ↑ | cAMP signaling pathway |
| (M + H) + | Thr-Lys | 1.323 | 7.172 | 3.49E−06 | 248.159 | ↑ | Others |
| (M + H) + | Trp-Phe | 1.626 | 5.652 | 4.17E−06 | 352.164 | ↑ | Others |
| $(M+H\text{-}H_2O)+$ | α-D-(+)-talose | 5.472 | 0.738 | 4.45E−06 | 163.060 | ↓ | Others |
| (M + H) + | Nicotinamide | 13.239 | 0.431 | 4.54E−06 | 123.055 | ↓ | Vitamin digestion and absorption |
| (M + H) + | 1-Palmitoyl-2-hydroxy-*sn*-glycero-3-phosphoethanolamine | 3.272 | 0.284 | 6.46E−06 | 454.292 | ↓ | Others |
| (M + H) + | Leu-Phe | 6.897 | 8.610 | 7.49E−06 | 279.169 | ↑ | Others |
| (M + H) + | Lys-Val | 1.808 | 5.690 | 8.41E−06 | 246.180 | ↑ | Others |
| (M + H) + | Xanthohumol | 2.680 | 3.111 | 9.67E−06 | 355.152 | ↑ | Flavonoid biosynthesis |
| (M + H) + | L-valine | 3.870 | 1.452 | 1.31E−05 | 118.086 | ↑ | ABC transporters |
| $(M+CH_3CN+H)+$ | *N*–ωhydroxyarginine | 1.752 | 7.768 | 1.56E−05 | 232.139 | ↑ | Arginine and proline metabolism |
| $(M+H\text{-}H_2O)+$ | DL-indole-3-lactic acid | 3.474 | 1.568 | 1.63E−05 | 188.070 | ↑ | Others |
| (M + H) + | Arg-Ala | 2.200 | 4.658 | 2.78E−05 | 246.155 | ↑ | Others |
| (M + H) + | Thr-Ile | 2.268 | 1.985 | 3.15E−05 | 233.148 | ↑ | Others |
| (M + H) + | L-carnitine | 7.045 | 0.284 | 4.16E−05 | 162.112 | ↓ | Thermogenesis |
| (M + H) + | Phe-Met | 1.466 | 4.684 | 4.43E−05 | 297.125 | ↑ | Others |
| (M + H) + | Stearidonic acid | 12.721 | 0.421 | 5.01E−05 | 277.216 | ↓ | Others |
| $(M+H\text{-}H_2O)+$ | 6-Aminocaproic acid | 2.016 | 0.568 | 7.08E−05 | 114.090 | ↓ | Microbial metabolism in diverse environments |
| (M + H) + | L-methionine | 2.181 | 2.378 | 7.34E−05 | 150.057 | ↑ | Glucosinolate biosynthesis |
| (M + H) + | Pantetheine | 1.725 | 0.651 | 9.99E−05 | 279.137 | ↓ | Pantothenate and CoA biosynthesis |
| (M + H) + | S-methyl-5′-thioadenosine | 3.782 | 2.121 | 1.22E−04 | 298.096 | ↑ | Cysteine and methionine metabolism |
| M + | (3-Carboxypropyl) trimethylammonium cation | 3.821 | 0.580 | 1.74E−04 | 146.117 | ↓ | Others |
| (M + H) + | Maltotriose | 2.188 | 1.284 | 2.23E−04 | 505.174 | ↑ | ABC transporters |
| $(M+NH_4)+$ | D-(-)-lyxose | 1.699 | 0.608 | 2.62E−04 | 168.086 | ↓ | Others |
| (M + H) + | Thr-Thr | 1.421 | 1.517 | 3.56E−04 | 221.112 | ↑ | Others |
| (M + Na) + | 16-Hydroxypalmitic acid | 7.124 | 0.309 | 5.19E−04 | 295.225 | ↓ | Cutin, suberine, and wax biosynthesis |
| (M + H) + | L-threonine | 1.556 | 3.972 | 7.01E−04 | 120.064 | ↑ | ABC transporters |
| $(M+NH_4)+$ | L-pyroglutamic acid | 4.086 | 0.235 | 7.85E−04 | 147.075 | ↓ | Glutathione metabolism |
| (M + H) + | 1-Palmitoyl-*sn*-glycero-3-phosphocholine | 2.104 | 0.211 | 8.16E−04 | 496.338 | ↓ | Others |
| (M + H) + | D-pipecolinic acid | 1.116 | 0.927 | 1.02E−03 | 130.085 | ↓ | Others |
| (M + H) + | Tryptamine | 2.609 | 1.952 | 1.35E−03 | 161.106 | ↑ | Indole alkaloid biosynthesis |
| $(M+CH_3CN+H)+$ | Val-Thr | 1.731 | 1.869 | 1.55E−03 | 260.159 | ↑ | Others |
| (M + H) + | Allopurinol riboside | 1.778 | 0.235 | 1.68E−03 | 269.087 | ↓ | Others |
| $(M+H\text{-}H_2O)+$ | Ornithine | 1.988 | 0.719 | 1.79E−03 | 115.086 | ↓ | Others |
| (M + H) + | Ile-Pro | 1.208 | 2.295 | 4.42E−03 | 229.154 | ↑ | Others |
| (M + H) + | L-leucine | 1.869 | 2.149 | 5.11E−03 | 132.101 | ↑ | mTOR signaling pathway |
| (M + H) + | Leu-Ser | 2.238 | 5.721 | 5.44E−03 | 219.133 | ↑ | Others |
| (M + H) + | *N*-acetylputrescine | 1.678 | 0.772 | 6.10E−03 | 131.117 | ↓ | Arginine and proline metabolism |
| $(M+H\text{-}2H_2O)+$ | 3–αMannobiose | 1.086 | 2.989 | 8.41E−03 | 307.101 | ↑ | Others |

**Table 1** (continued)

| Adduct | Description | VIP | Fold change | *p*-value | m/z | Trend | Functional category |
|---|---|---|---|---|---|---|---|
| (M + H) + | D-alanyl-D-alanine | 1.167 | 1.195 | 3.05E − 02 | 161.091 | ↑ | Peptidoglycan biosynthesis |
| (M-H)- | Ribothymidine | 2.074 | 0.125 | 6.83E − 11 | 257.078 | ↓ | Others |
| (M-H)- | Oleanolic acid | 2.136 | 8.822 | 2.99E − 10 | 455.351 | ↑ | Others |
| (M-H)- | Glycyl-L-leucine | 2.105 | 9.518 | 5.51E − 10 | 187.109 | ↑ | Others |
| (M-H)- | D-glucosamine 1-phosphate (glucosamine-1P) | 1.121 | 0.463 | 2.46E − 09 | 258.038 | ↓ | Amino sugar and nucleotide sugar metabolism |
| (M-H)- | L-glutamine | 2.915 | 0.321 | 4.65E − 09 | 145.062 | ↓ | ABC transporters |
| (M + $CH_3COO$)- | D-mannose | 14.889 | 1.995 | 9.92E − 09 | 239.078 | ↑ | ABC transporters |
| (M + $CH_3COO$)- | D-ribose | 1.101 | 2.410 | 1.15E − 08 | 209.067 | ↑ | ABC transporters |
| (M-H)- | 2′-Deoxyuridine | 1.578 | 0.352 | 1.34E − 08 | 227.067 | ↓ | ABC transporters |
| (M-H)- | Ribitol | 8.811 | 0.413 | 1.40E − 08 | 151.061 | ↓ | Pentose and glucuronate interconversions |
| (M-H)- | L-fucose | 2.560 | 0.465 | 1.72E − 08 | 163.061 | ↓ | Two-component system |
| (M + $CH_3COO$)- | Dulcitol | 6.530 | 0.476 | 1.06E − 07 | 241.093 | ↓ | Phosphotransferase system (PTS) |
| (M-H)- | L-saccharopine | 2.189 | 0.344 | 1.14E − 07 | 275.125 | ↓ | Lysine biosynthesis |
| (M-H)- | *N*-acetylglucosamine 1-phosphate | 1.952 | 0.480 | 4.09E − 07 | 300.049 | ↓ | Others |
| (M + $CH_3COO$)- | Ethosuximide | 1.347 | 0.364 | 4.98E − 07 | 200.093 | ↓ | Others |
| (M-H)- | 9-OxoODE | 15.018 | 0.223 | 1.03E − 06 | 293.212 | ↓ | Linoleic acid metabolism |
| (M + $CH_3COO$)- | Raffinose | 8.505 | 1.590 | 3.43E − 06 | 563.183 | ↑ | ABC transporters |
| (M-H)- | L-iditol | 1.160 | 0.542 | 4.27E − 06 | 181.072 | ↓ | Others |
| (M-H)- | L-tryptophan | 1.343 | 1.786 | 4.48E − 06 | 203.082 | ↑ | Indole alkaloid biosynthesis |
| (M-H)- | *N*-acetyl-L-alanine | 1.185 | 1.377 | 4.60E − 06 | 130.051 | ↑ | Others |
| (M + $CH_3COO$)- | D-fructose | 6.657 | 0.722 | 4.71E − 06 | 239.077 | ↓ | ABC transporters |
| (M-H)- | (S)-2-hydroxyglutarate | 1.988 | 0.479 | 1.23E − 05 | 147.030 | ↓ | Glucosinolate biosynthesis |
| M- | *N*-acetyl-D-lactosamine | 2.152 | 1.512 | 1.37E − 05 | 383.145 | ↑ | Others |
| (M-$H_2O$-H)- | Dihydroxyacetone | 1.480 | 1.311 | 1.90E − 05 | 71.014 | ↑ | Carbon metabolism |
| (M-H)- | Dihydrothymine | 1.267 | 0.313 | 2.35E − 05 | 127.051 | ↓ | Others |
| (M-H)- | L-glutamate | 2.362 | 0.330 | 2.39E − 05 | 146.046 | ↓ | Ferroptosis |
| (M-H)- | Caprylic acid | 1.117 | 1.409 | 2.58E − 05 | 143.108 | ↑ | Fatty acid biosynthesis |
| (M-H)- | Linoleic acid | 1.425 | 0.577 | 2.75E − 05 | 279.233 | ↓ | Linoleic acid metabolism |
| (M-H)- | *sn*-Glycerol 3-phosphoethanolamine | 2.214 | 0.678 | 4.29E − 05 | 214.049 | ↓ | Glycerophospholipid metabolism |
| (M-H)- | 2-Isopropylmalic acid | 1.420 | 0.236 | 6.57E − 05 | 175.061 | ↓ | Pyruvate metabolism |
| (M-H)- | 1-Palmitoyl-2-linoleoyl-*sn*-glycero-3-phosphate | 1.255 | 0.716 | 9.57E − 05 | 671.466 | ↓ | Others |
| (M-H)- | Heptadecanoic acid | 2.216 | 1.313 | 1.50E − 04 | 269.248 | ↑ | Others |
| (M-H)- | UDP-*N*-acetylglucosamine | 1.647 | 0.372 | 2.05E − 04 | 606.074 | ↓ | Peptidoglycan biosynthesis |
| (M-H)- | Uracil | 5.521 | 1.117 | 2.38E − 04 | 111.021 | ↑ | Pantothenate and CoA biosynthesis |
| (M-H)- | Glycolate | 2.050 | 0.688 | 3.76E − 04 | 75.009 | ↓ | Carbon metabolism |
| (M-H)- | Homogentisic acid | 1.557 | 0.489 | 4.35E − 04 | 167.035 | ↓ | Microbial metabolism in diverse environments |
| (M-H)- | DL-3-phenyllactic acid | 14.576 | 2.094 | 1.08E − 03 | 165.056 | ↑ | Biosynthesis of secondary metabolites |
| (M-H)- | Hydroxyisocaproic acid | 9.447 | 1.343 | 1.37E − 03 | 131.071 | ↑ | Others |
| (M-H)- | Succinate | 3.434 | 0.649 | 2.27E − 03 | 117.019 | ↓ | Citrate cycle (TCA cycle) |
| (M-H)- | Inosine | 3.060 | 0.184 | 2.90E − 03 | 267.074 | ↓ | ABC transporters |
| (M + Na-2H)- | 2′-Deoxy-D-ribose | 1.226 | 0.347 | 3.98E − 03 | 155.035 | ↓ | Pentose phosphate pathway |
| (M-H)- | 2-Hydroxy-3-methylbutyric acid | 3.659 | 1.292 | 5.10E − 03 | 117.055 | ↑ | Others |
| (M-H)- | Pentadecanoic acid | 1.742 | 0.870 | 9.99E − 03 | 241.217 | ↓ | Others |

**Table 1** (continued)

| Adduct | Description | VIP | Fold change | *p*-value | m/z | Trend | Functional category |
|---|---|---|---|---|---|---|---|
| (M-H)- | Thymine | 1.447 | 1.165 | 1.36E − 02 | 125.036 | ↑ | Pyrimidine metabolism |

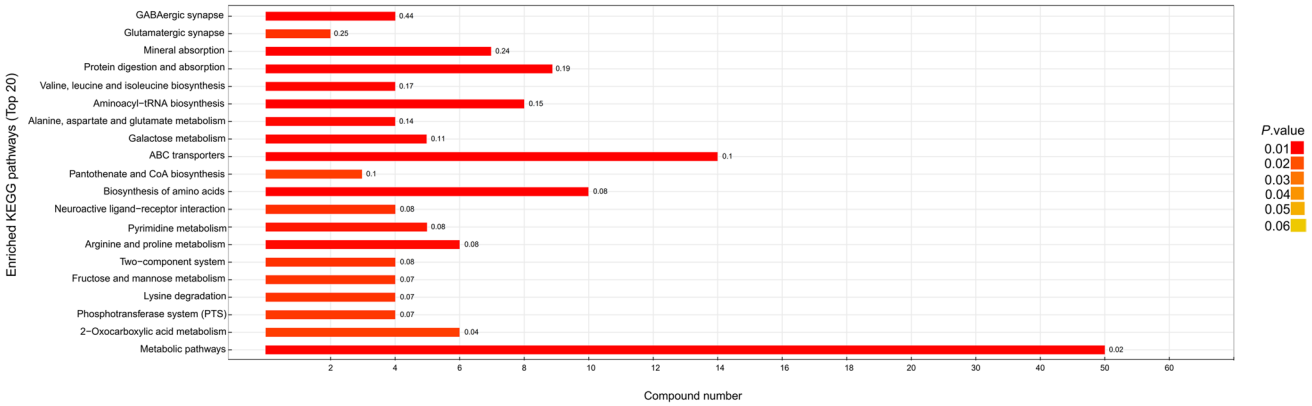


**Fig. 4** KEGG enrichment pathway diagram of the significantly differential metabolites between 1-nonanol-treated and untreated *A. flavus* mycelia

cause membrane disruption, enzyme inactivation, and cell apoptosis (Li et al. 2017, 2020; Cadenas and Davies 2000). The accumulation of $H_2O_2$ and superoxide anions in 1-nonanol-treated *A. flavus* cells indicates mitochondrial damage.

Apoptosis is a form of programmed cell death that is important for fungal development and homeostasis. Apoptosis occurs naturally in fungal cells during aging and reproduction and can be induced by environmental stresses (Hamann et al. 2008; Sharon et al. 2009). It involves multiple physiological changes in cells, including cell membrane damage, mitochondrial dysfunction, and DNA fragmentation (Elmore 2007). Excess ROS accumulation is a common response to fungal apoptosis (Hu et al. 2018; Madeo et al. 1999). Interestingly, we found that upregulated differential metabolites, *N*-ω-hydroxyarginine, *trans*-vaccenic acid, and oleanolic acid, might be involved in the induction of apoptosis of *A. flavus* exposed to 1-nonanol. These metabolites are involved in apoptosis in human cancers. *N*-ω-hydroxyarginine selectively inhibits cell proliferation and induces apoptosis in human breast cancer cells (Singh et al. 2000). Apoptosis of human nasopharyngeal carcinoma cells can be induced by *trans*-vaccenic acid through a mitochondrial-mediated apoptosis pathway (Song et al. 2019). Apoptosis in human hepatocellular carcinoma HuH7 cells can be induced by oleanolic acid through a mitochondrial-dependent pathway (Shyu et al. 2010). To our knowledge, the role of these three chemicals in fungal apoptosis had not been previously reported. The apoptosis-inducing effect of *N*-ω-hydroxyarginine, *trans*-vaccenic acid, and leanolic acid on *A. flavus* must be further studied. Besides, apoptosis involves multiple morphological and molecular changes in fungal cell. Recently, we found that hexanal treatment could induce apoptosis-related changes of physiological characteristics and key gene expression in *A. flavus* cells (Li et al. 2021a, b). However, the morphological and molecular characteristics of 1-nonanol-induced *A. flavus* apoptosis still need further investigation in our successive study.

Although 1-nonanol treatment caused damage to the cell membrane, disturbed the metabolic pathway, and induced apoptosis of *A. flavus*, the struggle for survival was observed in 1-nonanol-treated *A. flavus.* The reduction in ATPase activity in fungal cells is considered a resistance mechanism to decrease drug uptake (Nakamoto and Slayman 1989). In addition, the upregulated differential metabolites, tyramine, xanthohumol, and acetylcarnitine, might also be involved in the *A. flavus* resistance mechanism against 1-nonanol exposure. Tyramine can reduce cell division and reinforce cell wall strength in rice (Kim et al. 2011). Xanthohumol can ameliorate the induced cellular toxicity of 2,3,7,8-tetrachlorodibenzo-*p*-dioxin to MC3T3-E1 osteoblastic cells by reducing mitochondrial dysfunction and oxidative stress (Suh et al. 2018). Acetylcarnitine protects against apoptosis and aging of yeast cells by inhibiting mitochondrial fission (Palermo et al. 2010). These upregulated differential metabolites have a potential protective role in *A. flavus*, and their role will be investigated in future studies.

The potential applications of biogenic volatiles for the chemical control of fungal spoilage in postharvest agroproducts owing to their diffusibility, low toxicity, and high potency have been well documented (Brilli et al. 2019;

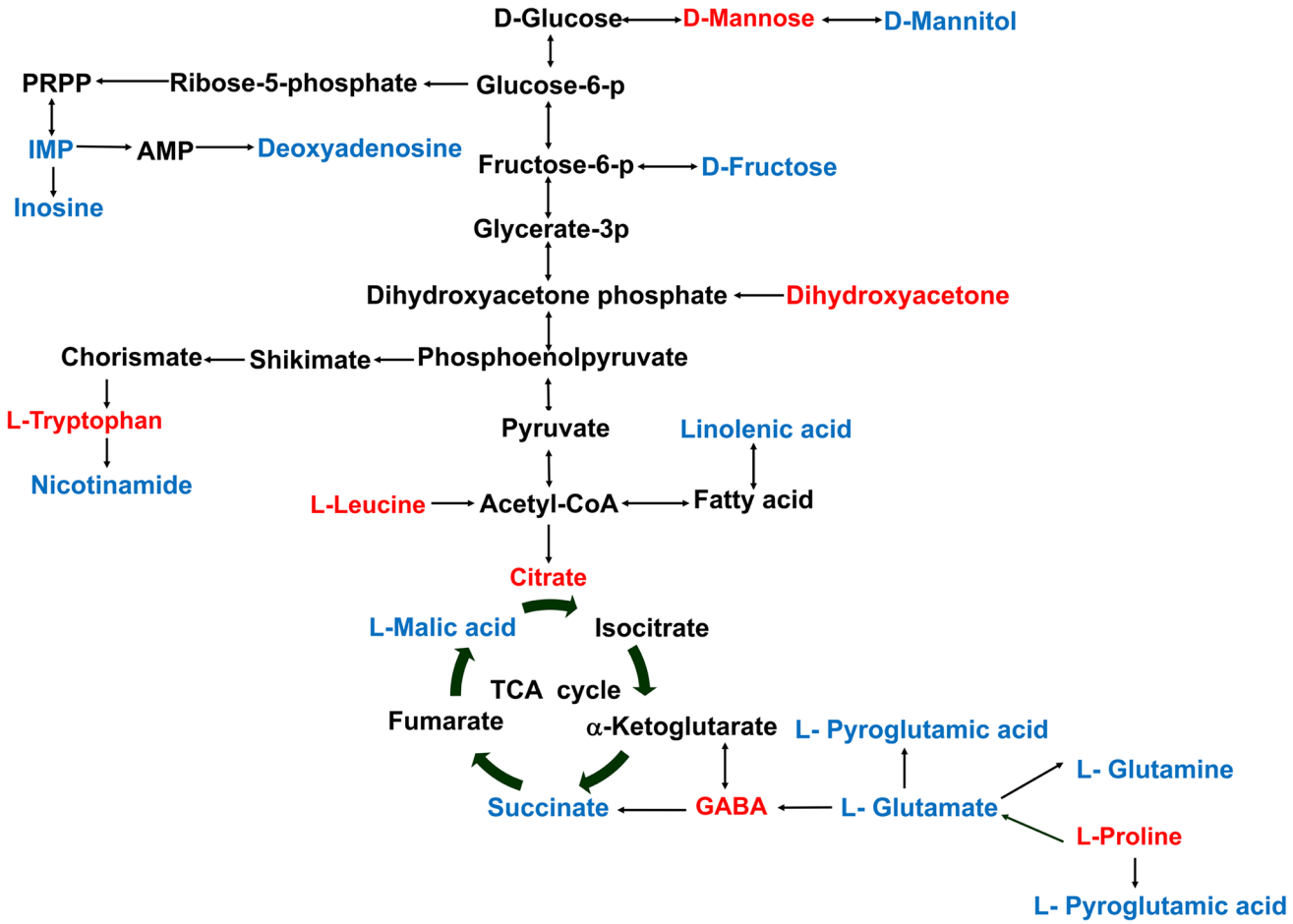


**Fig. 5** Biosynthetic pathways of selected upregulated (red color) and downregulated metabolites (blue color) in 1-nonanol-treated *A. flavus* mycelia obtained from the KEGG database

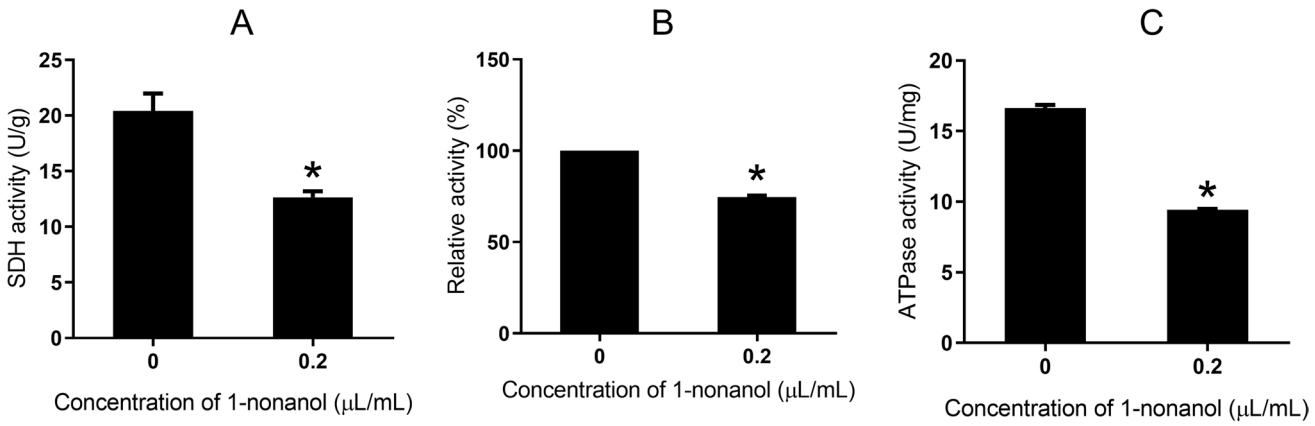


**Fig. 6** Comparison of SDH (**A**), mitochondrial dehydrogenase (**B**), and ATPase (**C**) activities between 1-nonanol-treated and untreated *A. flavus* mycelia. Data are presented as the mean ± SD ($n = 3$). The asterisk indicates significant differences, $p < 0.05$

Dukare et al. 2019; Kanchiswamy et al. 2015). Considering the need for consumption safety of cereal grains and their derived foods, authorized chemical preservatives are rarely used in postharvest grains (Fleurat-Lessard 2017). This concern might be overcome by the use of volatile compounds produced from cereal grains as preservatives.

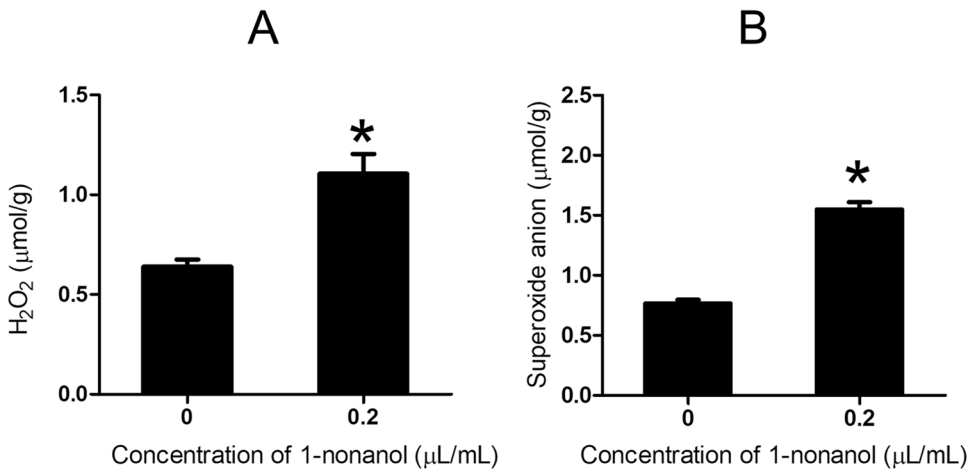


**Fig. 7** Comparison of $H_2O_2$ (**A**) and superoxide (**B**) anion levels between 1-nonanol-treated and untreated *A. flavus* mycelia. Values represent the mean ± SD ($n = 3$). The asterisk indicates significant differences, $p < 0.05$

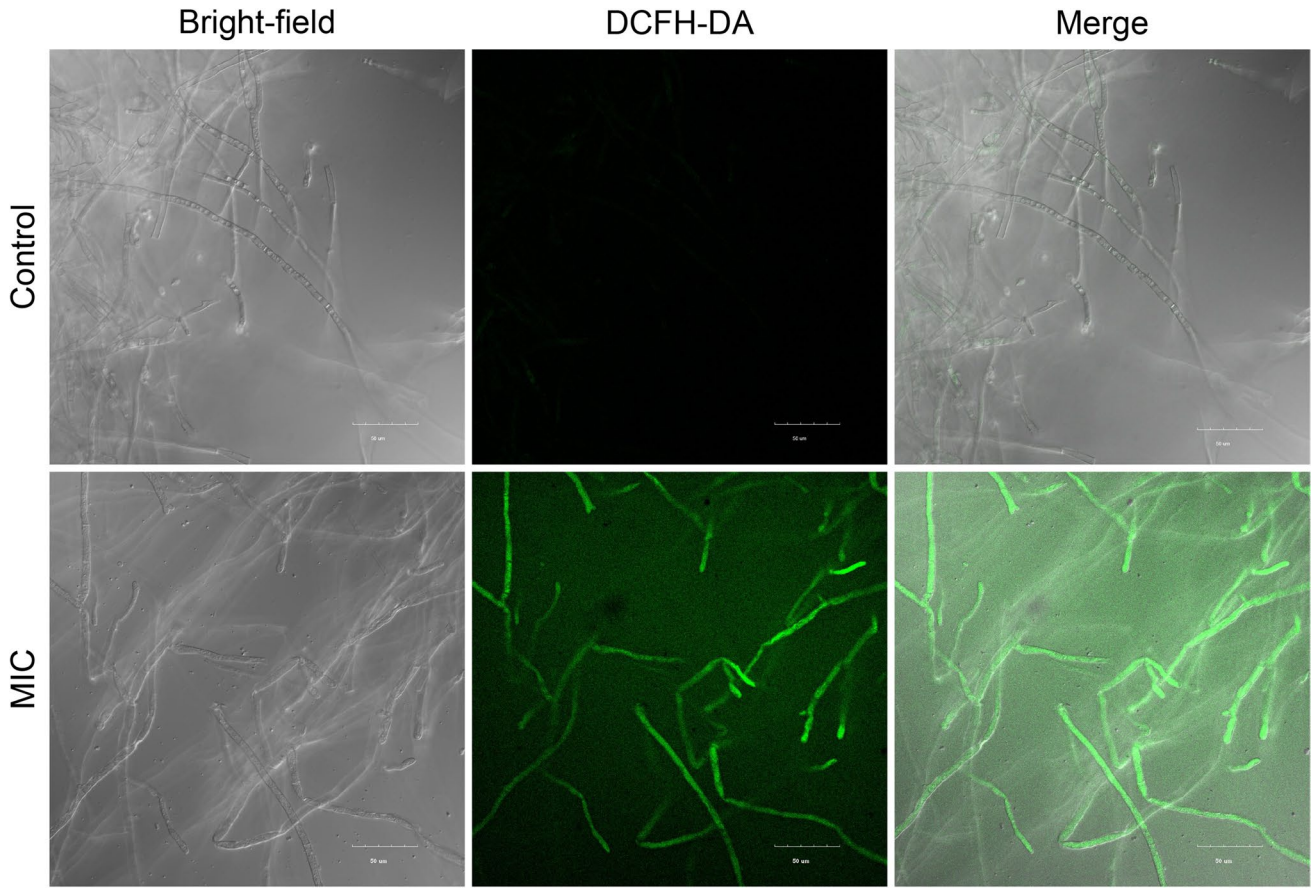


**Fig. 8** Fluorescence imaging of ROS accumulation in *A. flavus* hyphae after DCFH-DA treatment was observed by confocal laser scanning microscopy

The remarkable effectiveness of 1-nonanol in controlling the growth of *A. flavus* in wheat, corn, and paddy grains showed its great potential to control fungal spoilage of stored grains. As one of the main cereal volatiles, 1-nonanol vapor is diffusible and allows fumigation in large grain storage facilities. However, the effectiveness of 1-nonanol in controlling other spoilage fungi in stored grains and the effect of 1-nonanol residue on the grain process should be investigated further. We speculated that cereal volatiles might be a naturally evolved chemical defense mechanism of cereal grains against pathogenic diseases or pests (Zhang et al. 2021a). A few studies have supported this.

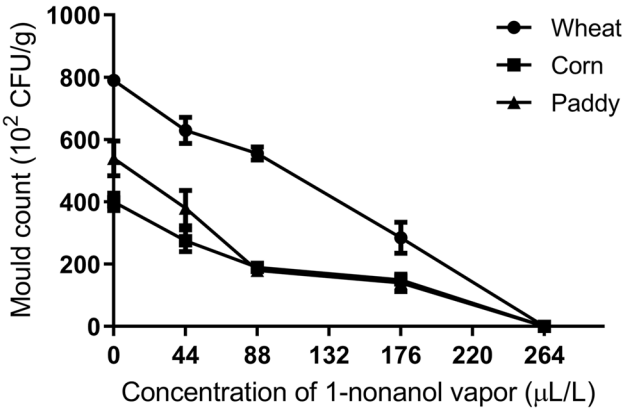


**Fig. 9** Mold counts in 18% moisture wheat, corn, and paddy grain fumigated with different concentrations of 1-nonanol after storage for 5 weeks at 28 ± 1 °C

Volatile aliphatic aldehydes, which disrupt the olfactory orientation of *Sitophilus granaries*, can be used as sustainable pest repellents in wheat grain (Germinara et al. 2015). Additionally, cereal volatile aldehydes inhibit the growth of *A. flavus* and aflatoxin production (Cleveland et al. 2009; Li et al. 2021a, b; Zhang et al. 2021a).

In this study, the growth of *A. flavus* was completely inhibited by exposure to 0.11 μL/mL 1-nonanol vapor or by 0.20 μL/mL liquid contact. Metabolomic analyses identified 135 significantly differential metabolites between the 1-nonanol-treated and untreated *A. flavus*. 1-Nonanol disrupts the permeability and integrity of the cytoplasmic membrane, TCA cycle, fatty acid, and amino acid metabolism and may induce apoptosis, resulting in cell membrane leakage, mitochondrial dysfunction, increased oxidative stress, and metabolic disorders in *A. flavus*. These effects were validated biochemically. We speculated that the 1-nonanol antifungal mechanism was mediated by the disruption of the cell membrane integrity and mitochondrial function and by the induction of apoptosis in *A. flavus* cells. The remarkable effectiveness of 1-nonanol in controlling the growth of *A. flavus* in cereal grains suggests that it is a promising bio-preservative for the prevention of fungal spoilage of postharvest grains, although other factors beyond its antifungal capability must be considered. The *A. flavus* apoptotic phenotype induced by 1-nonanol remains to be characterized in more detail.

**Supplementary Information** The online version contains supplementary material available at https://doi.org/10.1007/s00253-021-11581-8.

**Author contribution** SBZ obtained funding, conceived and designed the experiment, performed analysis, and wrote and revised the draft; YLQ performed experiments and wrote the original draft; SFL performed analysis and revised the draft; YYL performed analysis and editing; HCZ performed analysis and revised the original draft; YSH wrote the introduction section; JPC obtained funding and conceived and designed the experiment. All authors read and approved the manuscript.

**Funding** This work was supported by the National Key Research and Development Plan of China (grant number 2019YFC1605303-04), National Natural Science Foundation of China (grant number 31772023), Scientific and Technological Research Project of Henan Province (grant number 212102110193), Natural Scientific Research Innovation Foundation of Henan University of Technology (grant number 2020ZKCJ01), and Scientific Research Foundation of Henan University of Technology (grant number 2018RCJH14).

**Data availability** The datasets generated during and/or analyzed during the current study are available from the corresponding author on reasonable request.

## Declarations

**Ethics approval** This article does not contain studies conducted on human participants or animals by any of the authors.

**Conflict of interest** The authors declare no competing interests.

## References

Akram M (2014) Citric acid cycle and role of its intermediates in metabolism. Cell Biochem Biophys 68:475–478. https://doi.org/10.1007/s12013-013-9750-1

Basse CW (2010) Mitochondrial inheritance in fungi. Curr Opin Microbiol 13:712–719. https://doi.org/10.1016/j.mib.2010.09.003

Breitenbach M, Rinnerthaler M, Hartl J, Stincone A, Vowinckel J, Breitenbach H, Ralser KM (2014) Mitochondria in ageing: there is metabolism beyond the ROS. FEMS Yeast Res 14(1):198–212. https://doi.org/10.1111/1567-1364.12134

Brilli F, Loreto F, Baccelli I (2019) Exploiting plant volatile organic compounds (VOCs) in agriculture to improve sustainable defense strategies and productivity of crops. Front Plant Sci 10:264. https://doi.org/10.3389/fpls.2019.00264

Buttery RG, Ling LC, Chan BG (1978) Volatiles of corn kernels and husks: possible corn ear worm attractants. J Agric Food Chem 26(4):866–869. https://doi.org/10.3389/fpls.2019.00264

Cadenas E, Davies KJA (2000) Mitochondrial free radical generation, oxidative stress, and aging. Free Radic Biol Med 29:222–230. https://doi.org/10.1016/S0891-5849(00)00317-8

Cleveland TE, Carter-Wientjes CH, Lucca AJD, Boué SM (2009) Effect of soybean volatile compounds on *Aspergillus flavus* growth and aflatoxin production. J Food Sci 74(2):H83–H87. https://doi.org/10.1111/j.1750-3841.2009.01078.x

Dhakshinamoorthy D, Sundaresan S, Iyadurai A, Subramanian KS, Janavi GJ, Paliyath G, Subramanian J (2020) Hexanal vapor induced resistance against major postharvest pathogens of banana (*Musa acuminata* L.). Plant Pathol J 36(2):133–147. https://doi.org/10.5423/PPJ.OA.03.2019.0072

Dukare AS, Paul S, Nambi E, Gupta RK, Singh R, Sharma K, Vishwakarma RK (2019) Exploitation of microbial antagonists for the control of postharvest diseases of fruits: a review. Crit Rev Food Sci 59(9):1498–1513. https://doi.org/10.1080/10408398.2017.1417235

Elmore S (2007) Apoptosis: a review of programmed cell death. Toxicol Pathol 35(4):495–516. https://doi.org/10.1080/01926230701320337

Fleurat-Lessard F (2017) Integrated management of the risks of stored grain spoilage by seedborne fungi and contamination by storage mould mycotoxins: an update. J Stored Prod Res 71:22–40. https://doi.org/10.1016/j.jspr.2016.10.002

Germinara GS, Cristofaro AD, Rotundo G (2015) Repellents effectively disrupt the olfactory orientation of *Sitophilus granarius* to wheat kernels. J Pest Sci 88:675–684. https://doi.org/10.1007/s10340-015-0674-y

Gupta P, Gupta H, Poluri KM (2021) Geraniol eradicates *Candida glabrata* biofilm by targeting multiple cellular pathways. Appl Microbiol Biotechnol 1–17. https://doi.org/10.1007/s00253-021-11397-6

Hamann A, Brust D, Osiewacz HD (2008) Apoptosis pathways in fungal growth, development and ageing. Trends Microbiol 16(6):276–283. https://doi.org/10.1016/j.tim.2008.03.003

Hammerbacher A, Coutinho TA, Gershenzon J (2019) Roles of plant volatiles in defence against microbial pathogens and microbial exploitation of volatiles. Plant Cell Environ 42(10):2827–2843. https://doi.org/10.1111/pce.13602

He Y, Xu J, Wang X, He X, Wang Y, Zhou J, Zhang S, Meng X (2019) The arabidopsis pleiotropic drug resistance transporters PEN3 and PDR12 mediate camalexin secretion for resistance to *Botrytis cinerea*. Plant Cell 9:2206–2222. https://doi.org/10.1105/tpc.19.00239

Hu L, Ban F, Li H, Qian P, Shen Q, Zhao Y, Mo H, Zhou X (2018) Thymol induces conidial apoptosis in *Aspergillus flavus* via stimulating $K^+$ eruption. J Agric Food Chem 66(32):8530–8536. https://doi.org/10.1021/acs.jafc.8b02117

Kabak B, Dobson ADW, Var I (2006) Strategies to prevent mycotoxin contamination of food and animal feed: a review. Crit Rev Food Sci 46(8):593–619. https://doi.org/10.1080/10408390500436185

Kanchiswamy CN, Malnoy M, Maffei ME (2015) Bioprospecting bacterial and fungal volatiles for sustainable agriculture. Trends Plant Sci 20(4):206–211. https://doi.org/10.1016/j.tplants.2015.01.004

Kim YS, Park S, Kang K, Lee K, Back K (2011) Tyramine accumulation in rice cells caused a dwarf phenotype via reduced cell division. Planta 233:251–260. https://doi.org/10.1007/s00425-010-1303-x

Kubo I, Cespedes CL (2013) Antifungal activity of alkanols: inhibition of growth of spoilage yeasts. Phytochem Rev 12:961–977. https://doi.org/10.1007/s11101-013-9325-1

Li Y, Shao X, Xu J, Wei Y, Xu F, Wang H (2017) Tea tree oil exhibits antifungal activity against *Botrytis cinerea* by affecting mitochondria. Food Chem 234:62–67. https://doi.org/10.1016/j.foodchem.2017.04.172

Li Z, Shao X, Wei Y, Dai K, Wang H (2020) Transcriptome analysis of *Botrytis cinerea* in response to tea tree oil and its two characteristic components. Appl Microbiol Biotechnol 104:2163–2178. https://doi.org/10.1007/s00253-020-10382-9

Li S, Zhang S, Zhai H, Lv Y, Hu Y, Cai J (2021a) Hexanal induces early apoptosis of *Aspergillus flavus* conidia by disrupting mitochondrial function and expression of key genes. Appl Microbiol Biotechnol. https://doi.org/10.1007/s00253-021-11543-0

Li S, Zhang S, Lv Y, Zhai H, Li N, Hu Y, Cai J (2021b) Metabolomic analyses revealed multifaceted effects of hexanal on *Aspergillus flavus* growth. Appl Microbiol Biotechnol 105:3745–3757. https://doi.org/10.1007/s00253-021-11293-z

Liang D, Xing F, Selvaraj JN, Liu X, Wang L, Hua H, Zhou L, Zhao Y, Wang Y, Liu Y (2015) Inhibitory effect of cinnamaldehyde, citral, and eugenol on aflatoxin biosynthetic gene expression and aflatoxin $B_1$ biosynthesis in *Aspergillus flavus*. J Food Sci 80(12):M2917–M2924. https://doi.org/10.1111/1750-3841.13144

Ma W, Johnson ET (2021) Natural flavour (E, E)-2,4-heptadienal as a potential fumigant for control of *Aspergillus flavus* in stored peanut seeds: finding new antifungal agents based on preservative sorbic acid. Food Control 124:107938. https://doi.org/10.1016/j.foodcont.2021.107938

Madeo F, Fröhlich E, Ligr M, Grey M, Sigrist SJ, Wolf DH, Fröhlich K-U (1999) Oxygen stress: a regulator of apoptosis in yeast. J Cell Biol 145(4):757–767. https://doi.org/10.1083/jcb.145.4.757

Maffei ME, Gertsch J, Appendino G (2011) Plant volatiles: production, function and pharmacology. Nat Prod Rep 28:1359. https://doi.org/10.1039/c1np00021g

Magan N, Aldred D (2007) Post-harvest control strategies: minimizing mycotoxins in the food chain. Int J Food Microbiol 119:131–139. https://doi.org/10.1016/j.ijfoodmicro.2007.07.034

Mari M, Bautista-Baños S, Sivakumar D (2016) Decay control in the postharvest system: role of microbial and plant volatile organic compounds. Postharvest Biol Technol 122:70–81. https://doi.org/10.1016/j.postharvbio.2016.04.014

Mattiolo E, Licciardello F, Lombardo GM, Muratore G, Anastasi U (2017) Volatile profiling of durum wheat kernels by HS-SPME/GC-MS. Eur Food Res Technol 243:147–155. https://doi.org/10.1007/s00217-016-2731-z

Mohapatra D, Kumar S, Kotwaliwale N, Singh KK (2017) Critical factors responsible for fungi growth in stored food grains and nonchemical approaches for their control. Ind Crop Prod 108:162–182. https://doi.org/10.1016/j.indcrop.2017.06.039

Mukherjee K, Tribedi P, Mukhopadhyay B, Sil AK (2013) Antibacterial activity of long-chain fatty alcohols against mycobacteria. Fems Microbiol Lett 338:177–183. https://doi.org/10.1111/1574-6968.12043

Nakamoto RK, Slayman CW (1989) Molecular properties of the fungal plasma membrane $[H^+]$-ATPase. J Bioenerg Biomembr 21(5):621–632. https://doi.org/10.1007/BF00808117

Obianom C, Sivakumar D (2018) Natural plant volatiles as an alternative approach to control stem-end rot in avocado cultivars. J Phytopathol 166(1):1–9. https://doi.org/10.1111/jph.12653

Palermo V, Falcone C, Calvani M, Mazzoni C (2010) Acetyl-L-carnitine protects yeast cells from apoptosis and aging and inhibits mitochondrial fission. Aging Cell 9:570–579. https://doi.org/10.1111/j.1474-9726.2010.00587.x

Pichersky E, Noel JP, Dudareva N (2006) Biosynthesis of plant volatiles: nature's diversity and ingenuity. Science 311(5762):808–811. https://doi.org/10.1126/science.1118510

Qu S, Yang K, Chen L, Liu M, Geng Q, He X, Li Y, Liu Y, Tian J (2019) Cinnamaldehyde, a promising natural preservative against *Aspergillus flavus*. Front Microbiol 10:2895. https://doi.org/10.3389/fmicb.2019.02895

Rest MEVD, Kamminga AH, Nakano A, Anraku Y, Poolman B, Konings WN (1995) The plasma membrane of *Saccharomyces cerevisiae*: structure, function, and biogenesis. Microbiol Rev 59(2):304–322. https://doi.org/10.1006/mpat.1995.0038

Shao X, Cheng S, Wang H, Yu D, Mungai C (2013) The possible mechanism of antifungal action of tea tree oil on *Botrytis cinerea*. J Appl Microbiol 114(6):1642–1649. https://doi.org/10.1111/jam.12193

Sharon A, Finkelstein A, Shlezinger N, Hatam I (2009) Fungal apoptosis: function, genes and gene function. FEMS Microbiol Rev 33:833–854. https://doi.org/10.1111/j.1574-6976.2009.00180.x

Shyu M, Kao T, Yen G (2010) Oleanolic acid and ursolic acid induce apoptosis in HuH7 human hepatocellular carcinoma cells through a mitochondrial-dependent pathway and downregulation of XIAP. J Agric Food Chem 58(10):6110. https://doi.org/10.1021/jf100574j

Singh R, Pervin S, Karimi A, Cederbaum S, Chaudhuri G (2000) Arginase activity in human breast cancer cell lines: $N^w$-Hydroxy-L-arginine selectively inhibits cell proliferation and induces apoptosis in MDA-MB-468 cells. Cancer Res 60:3305–3312. https://doi.org/10.1002/pros.22698

Sipos G, Kuchler K (2006) Fungal ATP-binding cassette (ABC) transporters in drug resistance & detoxification. Curr Drug Targets 7(4):471–48. https://doi.org/10.2174/138945006776359403

Song J, Wang Y, Fan X, Wu H, Han J, Yang M, Lu L, Nie G (2019) *Trans*-vaccenic acid inhibits proliferation and induces apoptosis of human nasopharyngeal carcinoma cells via a mitochondrial-mediated apoptosis pathway. Lipids Health Dis 18:46. https://doi.org/10.1186/s12944-019-0993-8

Suprapta DN, Arai K, Iwai H (1997) Effects of volatile compounds on arthrospore germination and mycelial growth of *Geotrichum candidum* citrus race. Mycoscience 38(1):31–35. https://doi.org/10.1007/BF02464966

Suh KS, Choi EM, Kim HS, Park SY, Chin SO, Rhee SY, Pak YK, Choe W, Ha J, Chon S (2018) Xanthohumol ameliorates 2,3,7,8-tetrachlorodibenzo-*p*-dioxin-induced cellular toxicity in cultured MC3T3-E1 osteoblastic cells. J Appl Toxicol 38(7):1036–1046. https://doi.org/10.1002/jat.3613

Togashi N, Shiraishi A, Nishizaka M, Matsuoka K, Endo K, Hamashima H, Inoue Y (2007) Antibacterial activity of long-chain fatty alcohols against *Staphylococcus aureus*. Molecules 12:139–148. https://doi.org/10.3390/12020139

Víglaš J, Olejníková P (2021) An update on ABC transporters of filamentous fungi-from physiological substrates to xenobiotics. Microbiol Res 246:126684. https://doi.org/10.1016/j.micres.2020.126684

Wang N, Shao X, Wei Y, Jiang S, Xu F, Wang H (2020) Quantitative proteomics reveals that tea tree oil effects *Botrytis cinerea* mitochondria function. Pestic Biochem Phys 164:156–164. https://doi.org/10.1016/j.pestbp.2020.01.005

Wu Y, OuYang Q, Tao N (2016) Plasma membrane damage contributes to antifungal activity of citronellal against *Penicillium digitatum*. J Food Sci Technol 53:3853–3858. https://doi.org/10.1007/s13197-016-2358-x

Xu Y, Wei J, Wei Y, Han P, Shao X (2021) Tea tree oil controls brown rot in peaches by damaging the cell membrane of *Monilinia fructicola*. Postharvest Biol Technol 175:111474. https://doi.org/10.1016/j.postharvbio.2021.111474

Yang DS, Shewfelt RL, Lee K, Kays SJ (2008) Comparison of odor-active compounds from six distinctly different rice flavor types. J Agric Food Chem 56:2780–2787. https://doi.org/10.1021/jf072685t

Zhai H, Zhang S, Huang S, Cai J (2015) Prevention of toxigenic fungal growth in stored grains by carbon dioxide detection. Food Addit Contam A 32(4):596–603. https://doi.org/10.1080/19440049.2014.968221

Zhang S, Zheng M, Zhai H, Ma P, Lv Y, Hu Y, Cai J (2021a) Effects of hexanal fumigation on fungal spoilage and grain quality of stored wheat. Grain Oil Sci Technol 4:10–17. https://doi.org/10.1016/j.gaost.2020.12.002

Zhang W, Lv Y, Lv A, Wei S, Zhang S, Li C, Hu Y (2021b) Sub3 inhibits *Aspergillus flavus* growth by disrupting mitochondrial energy metabolism, and has potential biocontrol during peanut storage. J Sci Food Agric 101(2):486–496. https://doi.org/10.1002/jsfa.10657

Zhou M, Robards K, Glennie-Holmes M, Helliwell S (1999) Analysis of volatile compounds and their contribution to flavor in cereals. J Agric Food Chem 47(10):3941–3953. https://doi.org/10.1021/jf9904281